EDWARD YOST
SONDRA WENDEROTH
Long Island University
Greenvale, New York 11548

Multispectral Color for Agriculture and Forestry

A remote-sensing experiment demonstrated the ability to detect and identify tree species, crop types, crop maturation and range vegetation.

(*Abstract on next page*)

INTRODUCTION

DURING THE SUMMER OF 1967, a series of controlled experiments were performed to evaluate the usefulness of multispectral color aerial photography for obtaining quantitative data of interest to the disciplines of agriculture and forestry. The experiments were conducted using a four-lens multispectral camera and companion additive color viewer. This unique system was designed to obtain spectral photography in any four bands within the near-ultraviolet, visible, near-infrared region of the spectrum and to view the results in a single composite additive color presentation (Yost and Wenderoth, 1965, 1967). Three test sites were used: the Agricultural Experimental Test Station at Davis, California; the University of California Forestry Summer Camp at Bucks Lake, California; and the Rangeland Test Site at Harvey Valley, California. The project was a cooperative effort of the Science Engineering Research Group of Long Island University and the School of Forestry at the University of California, Berkeley.*

In addition to evaluating the resolution and chromatic image characteristics of multispectral color photography, the experiment had two other purposes. It was of interest to compare the relative accuracy of multispectral color photography with conventional subtractive color and color-infrared films. The possibility of obtaining unique signatures for species of agricultural crops and trees using this technique of combined abridged spectroradiometric remote sensing and colorimetric image analysis was also examined.

* This research was supported by the National Aeronautics and Space Administration under Contract NAS9-7291.

The Long Island University four-lens multispectral camera was used to obtain spectral photography at each test site. Simultaneous aerial Ektachrome and aerial Ektachrome infrared reversal color photographs were taken also. In order to facilitate the comparison of the characteristics of both the additive and subtractive color images, the spectral bands used in the multispectral camera were chosen to match the spectral sensitivities of the color film dye layers. Throughout the experiment, extensive ground control was used. This included gray-scale and color-target panels, measurement of the incident solar radiation spectra, spectroradiometric measurement of solar energy reflected by ground targets and colorimetric measurement of the target panels. The experiment was conducted at flight altitudes ranging from 1,000 to 30,000 feet above sea level. In order to include atmospheric effects, primary emphasis was given to the higher altitudes so so that the largest possible column of air would be placed between the ground and the camera.

Three types of problems were identified as being important considerations prior to the experiment. Firstly, the existence of unique spectral signatures for most environmental parameters of general ecological interest are not known at present. There is almost a complete absence of reliable spectra taken in situ. Dynamic variables in the environment such as variation of illumination, atmospheric attenuation, and preferential (non-lambertian) spectral reflectance of most natural objects exist. These variables tend to distort the underlying relationships between the energy reflected by an object and characteristics of the object which is being sought. Secondly, there conventionally exist large instrumenta-

tion errors such as variation in the spectral illumination in the focal plane of the sensor and a dependence of photographic density on the wave-length of radiation which often produce serious effects in photographic reproduction. These errors often obscure the subtle phenomena which one is attempting to detect. Thirdly, it is a physical fact that unique spectra produces a unique color, but the inverse is not true. It has been shown that the same color may be made by an infinite number of reflectance spectra (Evans, 1948). The technology of multispectral color photography is designed to circumvent this physical law of nature.

Experimental Procedures

The multispectral camera was equipped with four filters which were a combination of absorption and interference types which transmitted light in the following four spectral regions: blue (395–510 nm), green (480–590 nm), red (585–715 nm), infrared (700–900 nm). The film used was black-and-white infrared sensitive film (Kodak emulsion #5424). The log sensitivity of the film, the transmission of the filters given above, and the camera lenses as a function of wavelength are shown in Figure 1. The three filters used for the visible spectral bands were designed to block the transmission of all infrared radiation.

Two auxiliary K24 cameras were loaded with Aerial Ektachrome (Kodak emulsion #8442) and aerial Ekatchrome infrared (Kodak emulsion #8443) color reversal film. All cameras were aligned in a common mount in order that the optical axes would be parallel. The three cameras were actuated by a common intervalometer so that exposures were taken at the same time sithin the shutter tolerances of the three cameras.

Prior to flight, the multispectral camera was photometrically calibrated by using a set of gray scale panels under daylight illumination. The spectral distribution and intensity of the solar illuminant was measured simultaneously using a spectroradiometer. Since the percent directional reflectance of the gray scale target, as well as the camera shutter speed were known and constant, the solar power incident upon the scene in microwatts per centimeter squared could be related to the ergs per centimeter squared of image-forming energy striking the film in each band. Spectroradiometric monitoring of the incident solar energy while the aerial photography was being taken allowed (by using radio communication) control of the exposure in each band to be achieved throughout the day under both varying distribution and intensity of incident solar radiation.

Abstract: *The potential usefulness of multispectral color photography for the identification of crop and tree species has been demonstrated in a series of controlled experiments using broad-band camera filters which approximate the spectral sensitivity of color and color-infrared films. Independent adjustment of exposure in each camera band, control over the gamma and density of the photographic image, along with the ability to adjust the hue, brightness, and saturation in viewing, resulted in greater image chromatic separation than could be achieved using subtractive color reversal films. The capability to compensate for variations in the solar illuminant and atmospheric attenuation using additive color viewing of multispectral photographs was demonstrated.*

The negative infrared film was processed in a continuous Versamat processor using D-19 and developer. Sensitometric control was maintained. In general, a medium-to-high contrast was obtained on the negative although this varied depending on the condition encountered at a particular test site. Positive transparencies were made by duplicating on Kodak #5427 film using a Niagra printer and processing in a Versamat using MX 641 developer. Color films were processed using the rewind method, control strips being used to insure the best possible development within the state of that developing technique.

The positive images were placed in the additive color viewer. Numerous color spaces were experimentally formed in order to established those that gave the color differentiation that the interpreter considered best for his interests. The images of the ground targets and other objects were measured using a colorimeter. This data was compared with ground truth measurements made at the time the photography was taken. A similar analy-

sis was performed for substractive color films.

Photographic Considerations

The chromatic characteristics of the multispectral image which is formed by additive color methods are significantly effected by the photo processing techniques used. The relationship of exposure (or its radiometric equivalent, ergs per centimeter squared) to the density on both the negative film used in the camera and the positive transparency printed for projection in the viewer is a critical consideration.

If a multiband negative is properly exposed and processed to a gamma of 1.0, a one-to-one correspondence is created on the linear portion of the characteristic curve between the apparent color of ground objects objects and the density of the images on the film. Frequently, however, a gamma considerably greater than unity is necessary to differentiate chromatically objects that have nearly similar reflectance spectra. When a gray scale target which has uniform spectral reflectance is illuminated by a uniformly distributed source of radiation and photographed, the set of multispectral negatives which are produced should exhibit the same relative density characteristics in each spectral band. This exact matching of exposure and gamma is often difficult and frequently not possible, due to the effect of the wavelength of radiation which strikes the photographic emulsion. If one roll of film is used to expose all four spectral bands of distinctly different wavelengths, in general the characteristic curve associated with each band will be different. This effect is shown in Figure 2 in which the characteristic curves for infrared aerographic film exposed with the filters used in the experiment are plotted. The match in gamma therefore must be accomplished through differential printing of the positives.

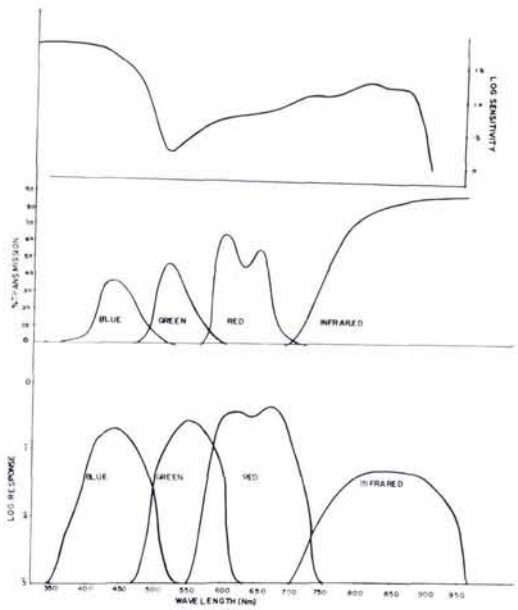

Fig. 1. Log sensitivity of Eastman Kodak infrared film #5424 is shown in the top figure. The selected filter transmissions are given in the center diagram, while the combination of filter-lens film response in each spectral band is shown in the lower figure.

A series of preliminary experiments were conducted in order to determine the effect of exposure and processing on the chromaticity of the additive color image. Four 100×100-foot color targets were placed on the ground along with five-step 40×40-foot calibrated gray scale panels (Data Corporation, 1969). It was possible to relate the density characteristics of the image directly to the brightness of the ground scene by comparing the image density on the positive with the reflection density of the gray scale.

Color images of the ground were constructed on the additive color viewer screen using the blue, green, and red spectral bands in order to form a true color reproduction of the color targets and the gray scale. Each of the sets of spectral positives used was processed and projected so that the gray scale target remained achromatic, i.e., without color. Curves of the gray scale reflection density and gray scale image density for each multispectral photograph were plotted and the associated gamma determined.

Color measurement of the chromaticity of the four color target images, along with the the white target image, is shown in Figure 3. Note how the color becomes more saturated (moves away from the center of the chromaticity diagram) as the gamma is increased. In all instances, the image of the white target has been placed at the same coordinate (*WH*) in the chromaticity diagram by manipulation of the viewer controls. In theory, all points should lie on a line from the center of the diagram. The deviations from a constant dominant wavelength as the gamma is increased are probably caused by slight variations in the shape of the characteristic curves for each spectral band. An often overlooked aspect of color reproduction is the effect that the minimum density has on the color of the image produced. The effect of reduced brightness as the minimum in density is increased while the gamma is kept constant results in

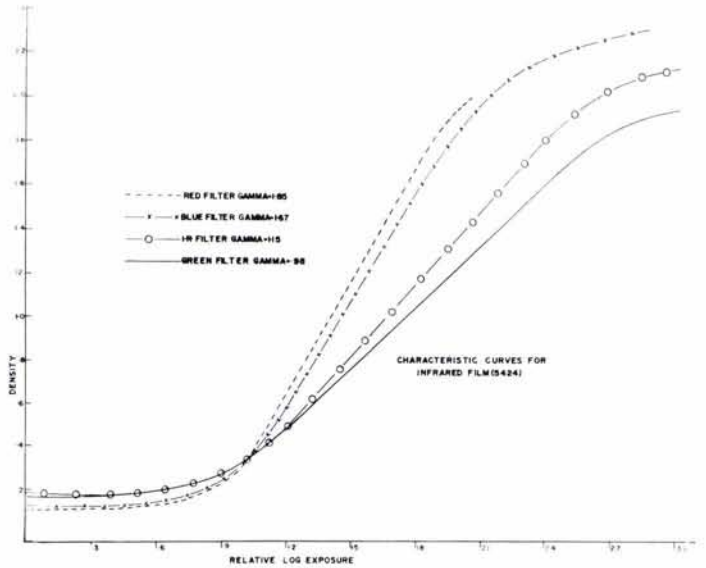

FIG. 2. Characteristic curves showing exposure-density relationships for the filters used in the experiment. The curves have been matched at .6 gamma in order to clearly show the different slope of the characteristic curve as a function of the spectral characteristics of the various filters.

reduced screen brightness and a consequent reduction in the perceived hue and saturation of the image (Anderson, 1969).

THE RESULTS OF THE EXPERIMENT

The multispectral color photographic system is designed for scientific analysis of remotely sensed spectral photography by viewing the composite additive color image projected on the viewer screen. Although consideredable care has been taken to make the color fidelity of these reproduced images as close as possible to that which was observed on the viewer screen, the reader should appreciate that it is not possible to achieve perfect reproduction in color printing.

AGRICULTURE

Four simultaneous positive photographs taken by the multispectral camera in the blue, green, red, and the infrared bands are shown in Figure 4. The photography was taken over the Agricultural Experimental Test Station, Davis, California at an altitude of 28,000 feet above sea level at 1200 Pacific Daylight Time on 31 July 1967. The scale of the original photography was approximately 1:44,000 and the ground truth is shown in Figure 5.

Many density differences can be detected between similar images in these four spectral photos. However, attempts to identify signatures of ground objects by multiple comparison of density differences on the four photographs is difficult and tedious at best.

By registered superimposition of the four photos in the additive color viewer, a composite color image is presented in which the

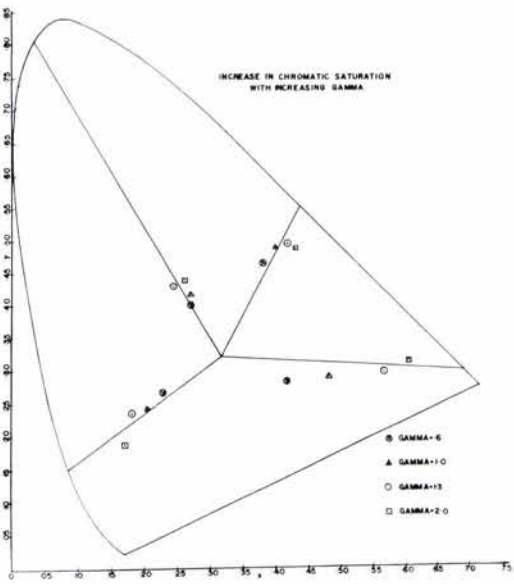

FIG. 3. The effect of gamma on saturation of the color of target panels on the ground is shown. Note how saturation increases with the increasing gamma for the blue, green, yellow, and red colors while the chromaticity coordinates of the white color remain unchanged.

density differences between the four photos appear as colors. Where no density differences exist, the image is a shade of gray. Using this method, the two hundred perceivable density differences are expanded into as many as ten million perceivable color differences (Nickerson and Newhall, 1943). Three of the many possible multispectral color renditions resulting from the projection of the photography are shown in the color plates which follow (Figures 7 through 10). The reproductions shown are multispectral color photographs produced by the additive color viewer from the four black-and-white spectral positives in Figure 4.

The large corn field (*C*) (Figure 5) can be seen (Figs. 9 and 10) to vary in color. This color change is related to the relative maturation of the crop which was five to six feet high at the top of the field and just sprouting in the bottom portion. This effect is difficult to detect in the visible color renditions (Figs. 7 and 8) although the demarcation of soil and foliage can be detected. The visible color renditions are useful in identifying plowed fields (*P*) from stubble (*S*). Variations in the productivity of tomatoes are shown by analysis of the areas (*E*) on Figures 7, 9 and 10 *E* (Figure 5) is a mature field of tomatoes in which variation in plant density indicates fertility differences in soil. E_2 is a plot planted later than E_1 in which the plants have completed flowering. The discoloration visible in Plate 4 results from standing irrigation water. The tomatoes in field E_3 are similar to E_2 but have not been irrigated for four days. E_4 is an immature field in which the plants have not yet flowered. Plots marked *N* show the colorimetric differentiation of beans; N_1 are mature plants and N_2 are recently sprouted plants from one-half to one foot high.

Alfalfa (*A*) is readily detected in both Figs. 8 and 9 as a homogeneous bright red color. However, in visible color renditions (Figs. 7 and 8) alfalfa appears quite similar to both corn and tomatoes. Beans and tomatoes grown in similar soil conditions and irrigated simultaneously in adjacent plots can be differentiated (*E*, *N*) in both the multiband color and infrared Ektachrome color renditions (Figs. 9 and 10). The characteristically bright red appearance of plot (*M*) in Figs. 9 and 10 indicates a patch of mature melons. The pasture (*PA*) can be identified by mottled appearance on infrared color photograph. Almonds (*AL*) and walnuts (*W*) are two groves which can be differentiated in color in both Figures 6 and 10 although quite similar in color in Fig. 8.

A comparison of the chromaticity coordinates of seven ground objects as they appear on Aerial Ektachrome Infrared subtractive photography and multispectral false-color rendition with the green band projected as blue, the red band as green, and the infrared band as red, is shown in Figure 6. It was observed by interpreters that it was possible to separate chromatically barley, milo, alfalfa, flowering tomatoes, and corn from each other *better* in the additive color presentation compared to the color infrared film images. The reader should notice the chromaticity coordinates of some images differ between the two color image-forming techniques. A bunching of the colors in the blue-magneta part of the diagram appears in the subtractive film images without the amount of chromatic separation that exists in the additive color multispectral presentation.

FORESTRY

An example of the determination of tree species is indicated in Fig. 12 which is a multispectral color photograph of the area adjacent to Bucks Lake, California. The photography was taken at an altitude of 28,000 feet above sea level at 1330 Pacific Daylight Time on 7 August 1967. The average scale is approximately 1:38,000. The associated ground truth data is presented in Figure 11. The following discussion is keyed to these annotations which can be referenced to the multispectral color photograph.

The distribution of four species of trees are readily identified by color difference on the multispectral photograph. California Black Oak (Quercus kelloggii) is indicated as bright orange (*A*); Riparian Hardwoods, principally White Alder appear as an orange red (*D*); Lodgepole Pine (Pinus contorta) is a dark magenta (*G*); White Fir (Abies concolor) appears as a dark red (*H*).

The spatial distribution of sedges and grass in a dry meadow is also clearly color differentiated (*C*). Variations in shades of pink are related to the vigor of the plants; cyan color is bare soil. The concentration of Manzanita brush cover in open fields can be directly contrasted to the sparseness of the same type of cover in the morains (*B*). The distribution of White Alder and Manzanita brush is readily identified as pink and red colors among the granitic outcrops (*E*) which appear as blue. The chromaticity coordinates of deciduous and coniferous trees, grass and rock appearing in Fig. 12 have been plotted in Figure 13. Note how coniferous and deciduous foliage are grouped in different parts of the

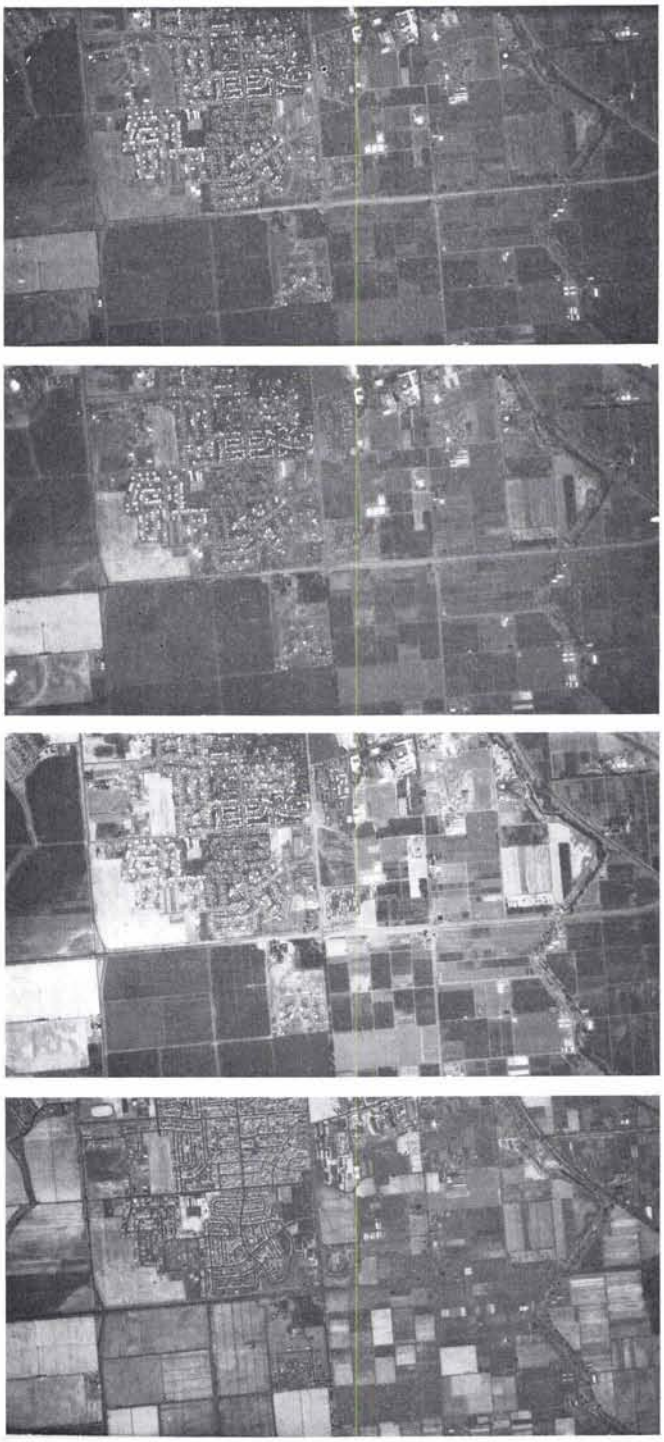

FIG. 4. Positive reproductions of four simultaneous photos taken by the multispectral camera. From top to bottom, the blue band records from 395 to 510 nm, the green band from 485 to 590 nm, the red band from 585 to 715 nm, and the infrared band from 700 to 900 nm.

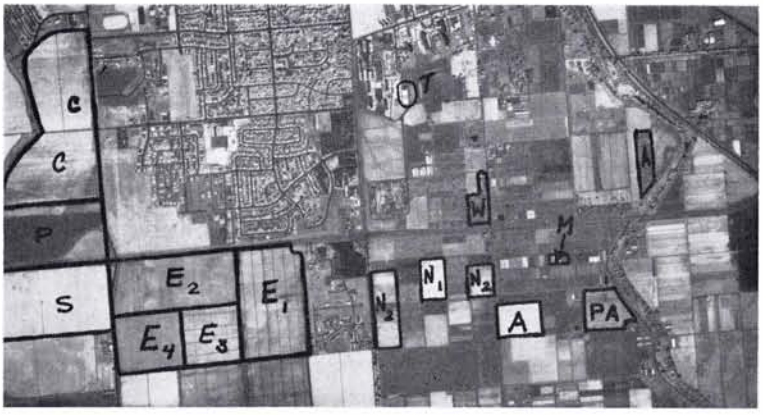

FIG. 5. Ground truth determined by the agricultural experiment station. (See Plates 1, 2, 3, 4). Legend: *C*, corn; *P*, plowed field; *S*, stubble field; E_1, mature tomatoes; E_2, tomatoes reaching maturity, recently irrigated; E_3, tomatoes just after flowering; E_4, tomatoes before flowering; N_1, mature beans, N_2, beans, recently sprouted; *A*, alfalfa, *PA*, pasture; *W*, walnuts; *Al*, almonds; *M*, melons; *T*, control targets

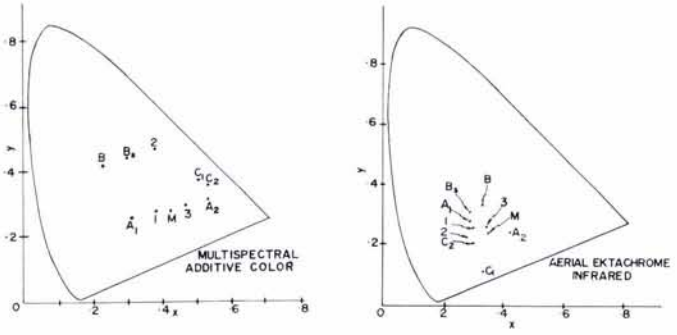

FIG. 6. A comparison of the chromaticity coordinates of crops appearing in multispectral false color (Plate 4) and Aerial Ektachrome infrared film (Plate 3). Legend: A_1, alfalfa (recently cut); A_2, alfalfa (mature), C_1, corn (mature); C_2, corn (new); *B*, barley, *BS*, bare soil; *1*, tomatoes (new plants); *2*, tomatoes (mature); *3*, tomatoes (after flowering).

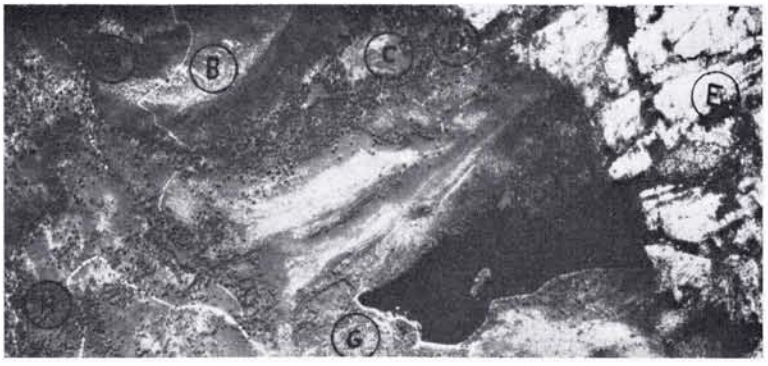

FIG. 11. Silver Lake. Legend: *A*, Quercus kelloggii (California Black Oak); *B*, glacial moraine (granitic) with sparse covering of Manzanita brush; *C*, dry meadow of sedges and grasses; *D*, riparian hardwoods (White Alder); *E*, granitic outcrop; *F*, large lake and smaller water bodies; *G*, Pinus contorta (Lodgepole Pine); *H*, Abies concolor (White Fir).

Figure 7. A multispectral true color rendition copied from the viewer screen in which the blue, green and red multispectral positives are projected each in the same color.

Figure 8. An aerial ektachrome photo taken at the same time as figure 7 using an optical system which is identical to that of the multispectral camera.

Figure 9. An aerial ektachrome infrared photograph of some agricultural crops exposed at 1617 PDT on 31 July 1967.

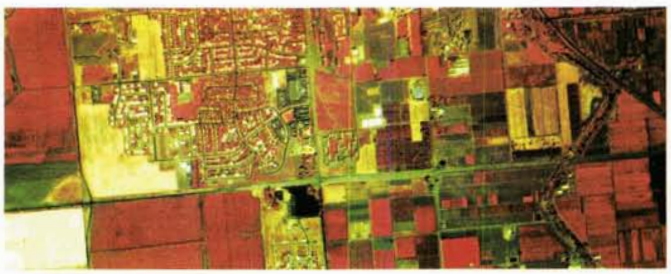

Figure 10. A multispectral rendition in which the green band is projected as blue, the red band projected as green, and the infrared band projected as red.

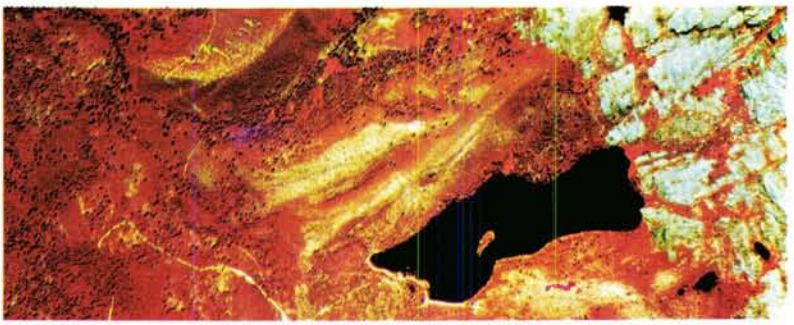

Figure 12. Silver Lake, California 28,000 feet above sea-level false color rendition. Green band projected as blue, red band projected as green, infrared band projected as red.

Figure 14. Serpentine area of Bucks Lake, California 28,000 feet above sea-level. The green band projected as blue, red band projected as red, the infrared band projected green.

Figure 16. Harvey Valley, California 28,000 feet above sea-level false color rendition. Green band projected as green, red band projected as red, and the infrared band projected as blue.

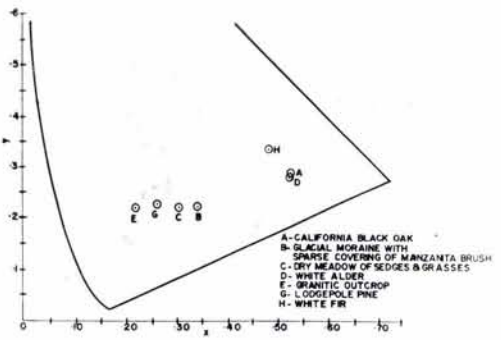

FIG. 13. Chromaticity coordinates of deciduous and coniferous trees, grass and rock shown in Figure 7.

chromaticity diagram. This indicates that these two classes of trees can be differentiated on the basis of image color. However, note that both California Black Oak and White Alder occupy nearly adjacent positions in the chromaticity diagram which indicates difficulty in chromatically differentiating these two types with the camera filters that were used in the experiment.

Figure 14 is a multispectral photograph of the Serpentine Area adjacent to Bucks Lake, California, which was taken at 1300 Pacific Daylight Time on 7 August 1967. The scale of photography is approximately 1:38,000. Figure 15 is an annotation of the photographs which shows data taken at different points on the ground.

Dense Riparian Hardwoods, predominantly Willow (Salix sp.) and a meadow of dry grass with scattered Willow can be identified (*B*). The distribution of the Willows has been correlated with the greater moisture in the stand and less soil moisture in the meadow. The moisture of the meadows (*D*) and (*E*) can be inferred by the density of cover of verdant meadow grasses. Meadow (*E*) contains greater soil moisture than (*D*) and both meadows (*D*) and (*E*) have greater average soil moisture than (*C*). The existence of lush grasses and sedges (Carex sp.) can be identified along with standing water in the wet meadow (*G*). Bare soil from a gold dredge tailing is shown (*I*) and the color can be related to progressive change in soil image color tones.

An example of open range land is shown in Figures 16 and 17. This area is Harvey Valley, California (lat. 40°41′N, long. 121°04′W) and was photographed at 1430 Pacific Daylight Time on 7 August 1967.

The distribution of meadow grasses particularly important for the supporting of range cattle can be inferred from the color variations in the multispectral presentation. The state of vigor of rushes and sedges (Carex sp.) can be identified with receding water after winter (*1* and *2*, Figure 16). Dense stands of sedges in standing water can be detected by the color differences. Low sage brush growing on light toned soil is related to the light brown color (*3*). This type of covering can be differentiated from a reseeded area of Bromus inermus grass (*4*) which has a darker color. The potential productivity of the two areas for grazing forage is greater for area *4* than area *3*.

The presence of dense, lush meadow vegetation, predominately sedges, forbs, and some water-loving grasses (*5*), indicates high productivity of this forage area. Big sagebrush sites (*6*) can be identified by change in

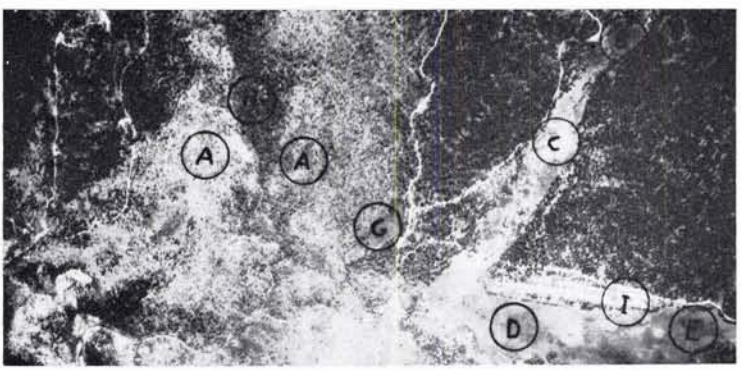

FIG. 15. Serpentine area. Legend: *A*, Dubakella soil, ground cover is Ceanothus cuneatus (backbrush); *B*, riparian hardwood vegetation predominately Salix sp. (Willow); *C*, meadow of dry grass with some scattered Salix sp.; *D*, meadow with a higher proportion of green vegetation; *E*, very moist meadow area; *F*, dense stand of mixed conifers on Cohassett soil; *G*, wet meadow, lush grasses, and sedgex (Cares Sp.); *H*, fairly dense stand of timber of Dubakella soil; *I*, bare gravel—gold dredge tailing from early mining operations.

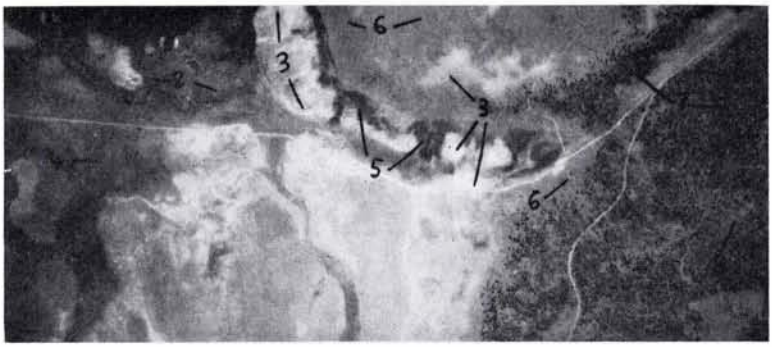

FIG. 17. Harvey Valley. Legend: *1*, integration of standing water in and among a dense stand of sedges (Carex sp.); *2*, partially dried rushes and sedges; *3*, low sagebrush type; *4*, Bromus inermus grass; *5*, very dense, lush meadow vegetation in which the dominant species include sedges, forbs; *6*, big sagebrush sites; 7, Ponderosa Pine; *8*, Manzanita brushfield.

brightness as compared to low sagebrush types of cover (*3*). Big sagebrush covers about 20% of the ground surface and grows in reddish-brown soils up to three feet deep. Stands of Ponderosa Pine can be readily identified (*7*) as is the Manzanita brushfield which has come into the forested area following a burn (*8*).

Environmental Measurements

The amplitude and wavelength of electro magnetic radiation in the visible and near-infrared portion of the spectrum which is reflected by the environment constantly varies with both solar angle and atmospheric conditions. Objects on the ground reflect varying amounts of this radiation at every wavelength not only in proportion to that falling upon them but also as a function of environmental variables which dynamically change their absorption, transmission, and reflectance characteristics.

Figure 18 is a graph of the spectral distribution of solar radiation taken at Davis, California, on 31 July 1967 using a spectroradiometer with a lambertian (cosine) detector surface. The large variation in microwatts per centimeter squared per nanometer of total sunlight and diffuse skylight falling upon the ground at different times during the day is clearly evident. This graph also shows that at this particular place and time there was a large increase in infrared radiation present in sunlight at 750 nanometers in the afternoon compared to the morning. This is probably due to the absorption of light by large dust particles which have been churned up in the fields during the day. The ability to control the exposure independently in each spectral band gives the multispectral camera the ability to compensate for this dynamic variable in the environment. Color-infrared film, on the other hand, seemed to be slightly more red in the afternoon compared to the morning which can be attributed to the fixed sensitivity of the individual dye layers.

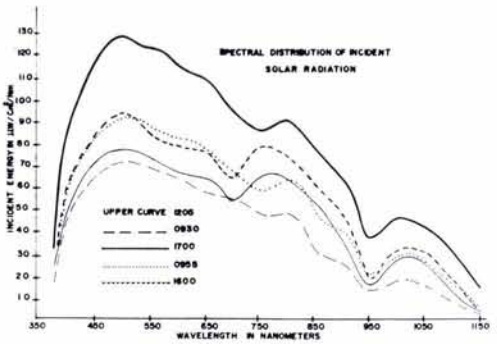

FIG. 18. Variation in the intensity and distribution of solar radiation incident upon the ground with time of day (solar angle) as well as with atmospheric conditions.

There is one aspect of solar illumination that cannot be compensated by variation in exposure in the multispectral camera. This is the spectral difference between the solar radiation falling directly on the ground and the diffuse skylight that illuminates shadow areas. Figure 19 shows a comparison of direct sunlight and diffuse skylight made at the same time on 30 July 1967 at Davis, California. In addition to the obvious reduction in intensity, skylight is predominantly blue which results in an apparent increase in the relative amount of radiation reflected in the blue band compared to other bands when an object is in the shade.

Any remote sensing instrument is a perspective sensor. It views an object on the

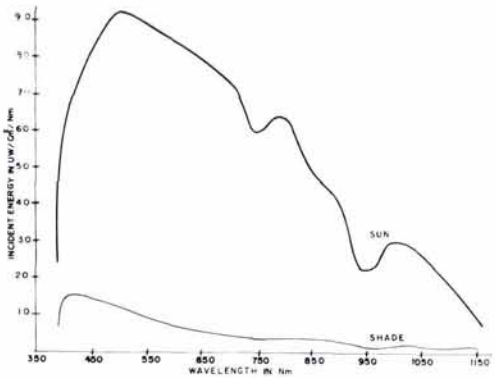

FIG. 19. The spectral intensity and distribution of direct solar radiation and diffuse skylight which illuminates shadows is different.

ground at a specific angle which depends on both the orientation of the object and the orientation of the sensor. Each image on a photograph thus is *seen* at different perspective. Solar radiation also falls on surface objects at varying angles of incidence depending on both the time of day and the orientation of the object. The question arises, "What effect do these angular relationships have on the spectra of an object as recorded by the sensor?"

Figure 20 demonstrates this important and unresolved problem. A gray target was specially constructed to present a diffuse surface which was measured in the laboratory using a spectrophotometer with a total diffusing sphere. In the field, a spectroradiometer was employed to measure the incident sun and skylight falling onto the gray panel. The percentage of incident radiation which was reflected by this *diffuse* gray panel is quite different from the total diffuse reflectance calibration made in the laboratory. The field

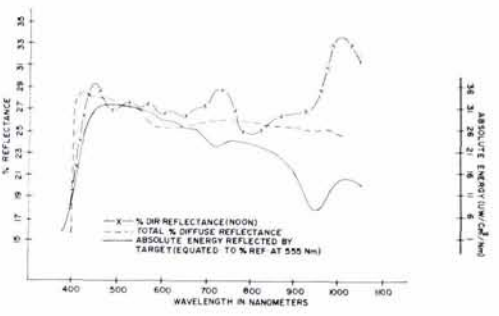

FIG. 20. Comparison of the spectrophotometric total diffuse reflectance and percentage reflectance under natural illumination in the direction of the camera and the relative distribution of the energy actually reflected.

measurements were taken using a spectroradiometer which was oriented at a 30°-angle with respect to the surface normal and 90° in azimuth from the direction of the sun. The actual amount of solar radiation reflected by the target in the direction of this orientation, which would be the power *seen* by a remote sensor in the same orientation, is shown in the solid curve of Figure 20. This curve shows the target spectra which results when the combined effect of the spectral distribution and intensity of sunlight is considered along with the directional reflectance characteristics of the target.

The chromaticity of four color panels was measured on the ground at the time multispectral photographs were taken. These color coordinates are shown in Figure 21. In addition, the colors of the images of the panels as they appeared on the viewer screen and on Ektachrome color film were also measured. Note how closely the additive color image can be made to match the actual color of the object. Although the chromaticity coordinates appear close to the white point, it should be emphasized that the brightness levels of the panels varied between 21 and 42 percent; low brightness causes a compression of the color space toward white or gray.

CONCLUSIONS

A remote-sensing experiment was conducted which demonstrated the usefulness of

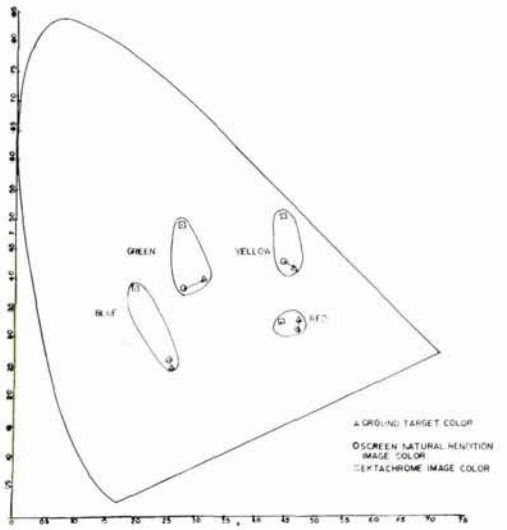

FIG. 21. A comparison of the chromaticity coordinates of blue, green, yellow, and red target panels measured on the ground with the color of images of the panels as they appear on multispectral additive color viewer screen and on aerial Ektachrome subtractive reversal film.

multispectral color aerial photography for agricultural and forestry applications. The ability to detect and identify basic parameters such as tree species, crop types, crop maturation and range vegetation using broad-band camera filters which were not designed specifically for the task is most significant. Elimination of the gross instrumentation errors which have previously plagued the technology of multispectral photography has been achieved. The effects of environmental variables on the color characteristics of multispectral images, particularly that caused by variation of the incident solar radiation during the day, have been reduced. We are beginning to understand the cause of spectral errors resulting from perspective as well as these effects on the multispectral images.

Spectroradiometric reflectance data collected during the experiment appears to be helpful in detecting differences among crop and tree species. Particularly subdivision of the spectral band from 680–900 nm seems to offer promise for establishing unique chromatic differences in the images of living vegetation.

The ability to make color images closely match the actual colors of objects as they exist in situ, and correcting the distortion in image color caused by variations in solar illumination and atmospheric attentuation, is promising when it is desired to establish and classify an object by its true color.

ACKNOWLEDGEMENTS

The ground truth and environmental measurements obtained during the experiment were made by William Press of Long Island University and the following personnel from the School of Forestry at the University of California, Berkeley: William Dreager, Eric Janes, Jerry Lent, Larry Pettinger, John Thomas, and Gene Thorley.

REFERENCES

Anderson, R. (1969): "The Parameters of Color Reproduction in Additive Color Aerial Photography". Proceedings of the seminar *New Horizons in Color Aerial Photography*, American Society of Photogrammetry.

Data Corporation (1969): *CORN Target Manual*, revised 23 April 1969.

Evans, R. (1948): *An Introduction to Color*, Wiley.

Maxwell, J. C. (1960): "On the Theory of Compound Colours and the Relations of the Colours of the Spectrum". *Proceedings of the Royal Society*, London, Vol. 10, pp. 404.

Nickerson and Newhall (1943): "A Psychological Color Solid". *Journal of the Optical Society of America*, Vol. 33, pp. 419.

Yost, E. and S. Wenderoth (1965): "The Chromatic Characteristics of Additive Color Aerial Photography". *Science and Engineering*, Vol. 9, No. 3.

Yost, E. and S. Wenderoth (1967): "Multispectral Color Aerial Photography". *Photogrammetric Engineering*, Vol. 33, pp. 1020.

Yost, E. and S. Wenderoth (1968): "Additive Color Aerial Photography" in the *Manual of Color Aerial Photography*, J. Smith, editor, American Society of Photogrammetry.

Notice to Contributors

1. Manuscripts should be typed, double-spaced on $8\frac{1}{2}\times11$ or $8\times10\frac{1}{2}$ white bond, on *one* side only. References, footnotes, captions—everything should be double-spaced. Margins should be $1\frac{1}{2}$ inches.
2. *Two* copies (the original and first carbon) of the complete manuscript and two sets of illustrations should be submitted. The second set of illustrations need not be prime quality.
3. Each article should include an abstract, which is a *digest* of the article. An abstract should be 100 to 150 words in length.
4. Tables should be designed to fit into a width no more than five inches.
5. Illustrations should not be more than twice the final print size: *glossy* prints of photos should be submitted. Lettering should be neat, and designed for the reduction anticipated. Please include a separate list of captions.
6. Formulas should be expressed as simply as possible, keeping in mind the difficulties and limitations encountered in setting type.